ARTICLE

Aberrant promoter hypermethylation inhibits RGMA expression and contributes to tumor progression in breast cancer

Yan Li [1,2,3], Hai-Ting Liu[1,2], Xu Chen[1,2], Ya-Wen Wang[1,2], Ya-Ru Tian[1,2], Ran-ran Ma[1,2], Lin Song[1,2], Yong-Xin Zou [2✉] and Peng Gao [1,2✉]

Breast cancer (BC) is the most common cancer in women worldwide, and the exploration of aberrantly expressed genes might clarify tumorigenesis and help uncover new therapeutic strategies for BC. Although RGMA was recently recognized as a tumor suppressor gene, its detailed biological function and regulation in BC remain unclear. Herein, we found that RGMA was downregulated in BC tissues compared with non-tumorous breast tissues, particularly in metastatic BC samples, and that patients with low RGMA expression manifested a poorer prognosis. Furthermore, DNMT1 and DNMT3A were found to be recruited to the RGMA promoter and induced aberrant hypermethylation, resulting in downregulation of RGMA expression in BC. In contrast, RGMA overexpression suppressed BC cell proliferation and colony-formation capabilities and increased BC cell apoptosis. Furthermore, RGMA knockdown accelerated BC cell proliferation and suppressed cellular apoptosis in vitro and in vivo. Reversal of RGMA promoter methylation with 5-Aza-CdR restored RGMA expression and blocked tumor growth. Overall, DNMT1- and DNMT3A-mediated RGMA promoter hypermethylation led to downregulation of RGMA expression, and low RGMA expression contributed to BC growth via activation of the FAK/Src/PI3K/AKT-signaling pathway. Our data thus suggested that RGMA might be a promising therapeutic target in BC.

INTRODUCTION

Breast cancer (BC) is the most commonly diagnosed malignancy and the leading cause of cancer-related deaths among women worldwide [1]. Despite the recent advances in comprehensive therapies for BC, its prognosis remains unsatisfactory. The tumorigenic and malignant progression of BC is tightly associated with genetic and epigenetic mechanisms [2, 3], and it is therefore essential to explore the relevant underlying molecular mechanisms and uncover novel therapeutic targets so as to improve the efficacy of BC-treatment strategies.

Repulsive guidance molecule A (RGMA), a glycosylphospha tidylinositol-anchored cell membrane-associated protein primarily functions in the central nervous system, regulates axonal guidance and neural differentiation and plays a crucial role in autoimmune encephalomyelitis and Parkinson's disease [4–6]. Accumulating evidence has demonstrated that RGMA, together with its associated receptor, is linked to the pathogenesis of carcinogenesis, including prostate cancer, colon cancer, and oral squamous cell carcinoma [7–9]. Investigators previously reported that methylation was the predominant mechanism subserving the downregulation of RGMA in colon cancer, and methylation-specific PCR (MSP) analysis showed that RGMA was frequently silenced by promoter methylation in colon cancer tissues, adenomas, and colon cancer cell lines but not in normal colonic tissues. 5-Aza-CdR treatment restored RGMA expression in colon cancer cell lines [10], and high RGMA expression inhibited cancer cell migration and angiogenesis by downregulating VEGF [11]. Xiao et al. reported that high expression of RGMA was significantly associated with improved luminal BC prognosis [12], and in our previous study, we demonstrated that RGMA served as a target gene of miR-4472, a metastasis-promoting miRNA. Downregulation of RGMA by miR-4472 accelerates BC aggressiveness via the epithelial-to-mesenc hymal transition [13], indicating that silencing of RGMA might be involved in tumorigenesis. Moreover, RGMA shows frequent hypermethylation in the promoter region in colon cancer [10]. However, there are no detailed studies published on the methylation status and governing molecular mechanisms with respect to RGMA in BC.

In the present study, low expression of RGMA was associated with malignant growth and a poorer prognosis, and we showed that RGMA functioned as a tumor suppressor in BC. DNMT1- and DNMT3A-mediated promoter hypermethylation also resulted in the downregulation of RGMA expression. Furthermore, RGMA inactivated the FAK/Src/PI3K/AKT-signaling pathway to suppress tumor progression in BC. Our study thus revealed a novel role for RGMA in suppressing BC growth, which might provide a potential therapeutic strategy for BC treatment.

[1]Department of Pathology, Qilu Hospital of Shandong University, Jinan 250012 Shandong, China. [2]Key Laboratory for Experimental Teratology of Ministry of Education, Department of Pathology, School of Basic Medical Sciences, Cheeloo College of Medicine, Shandong University, Jinan 250012 Shandong, China. [3]Department of Gastroenterology, Qilu Hospital (Qingdao), Shandong University, Qingdao 266035 Shandong, China. ✉email: zouyongxin@sdu.edu.cn; gaopeng@sdu.edu.cn

RESULTS

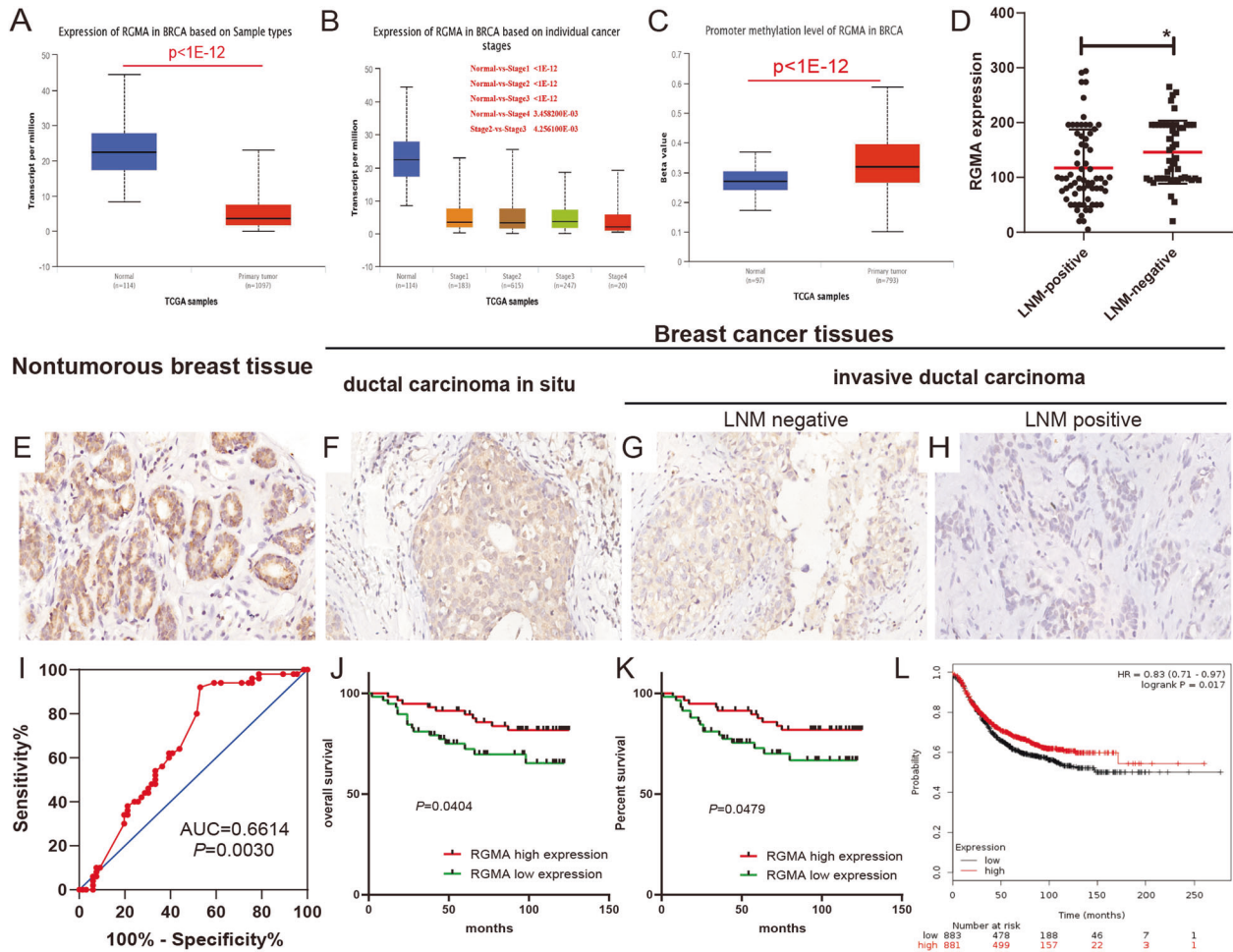### The expression of RGMA is downregulated in BC tissues, particularly in metastatic BC tissues

We first used the publicly available UALCAN web-tool to analyze the expression of RGMA in BC and noted that RGMA mRNA levels were significantly downregulated in BC tissues compared to normal mammary samples (normal, $n = 114$; tumor $n = 1097$; Fig. 1A) and the expression level of RGMA decreased commensurately with advanced tumor stage (Fig. 1B). In addition, the *RGMA* promoter methylation level was significantly elevated in primary BC tissues relative to normal tissues (Fig. 1C).

We then investigated a cohort of 116 Chinese women with BC at our hospital (the Qilu 116 BC cohort) by immunohistochemistry (IHC) and observed cellular staining for RGMA in both the membrane and the cytoplasm. IHC results revealed that RGMA displayed weaker expression in BC tissues than in nontumorous breast tissues and that the expression exhibited a gradual diminution from nontumorous breast tissues via ductal carcinoma in situ to invasive ductal carcinoma. Intriguingly, RGMA expression in lymph-node metastasis (LNM)-positive BC tissues was significantly attenuated compared to LNM-negative tissues (Fig. 1D–H). These results suggested that RGMA could be a tumor suppressor gene in BC.

RGMA is associated with clinicopathological parameters and a favorable prognosis in BC patients

We explored the correlation between RGMA expression and a series of clinicopathological characteristics that included age, tumor size, lymph node metastases, pathological tumor node metastasis (pTNM) grade, status of estrogen receptor (ER), status of progesterone receptor (PR), and human epidermal growth factor receptor-2 (HER2), and the molecular classification used on the data from the 116 patients. Analysis of the clinicopathological parameters demonstrated much lower expression of RGMA in LNM-positive tissues relative to LNM-negative tissues. Moreover, augmented RGMA expression was significantly correlated with earlier T stage and positive ER and PR status (Table 1). Furthermore, receiver operator characteristic (ROC) curves showed that RGMA expression could be used to distinguish patients with or without LNM, with an area under the ROC curve (AUC) of 0.6614 (Fig. 1I).

Fig. 1 RGMA was downregulated in BC. A RGMA expression was significantly downregulated in BC tissues compared with normal mammary tissues from TCGA databases using UALCAN. **B** The UALCAN database showed that RGMA expression was significantly correlated with tumor grades. As tumor grades increased, the expression of RGMA tended to be lower. **C** The UALCAN database showed that RGMA methylation level was elevated in primary BC tissues relative to normal tissues. **D** RGMA expression was downregulated in lymph-node-metastasis (LNM) -positive cancer tissues compared to LNM-negative tissues in 116 BC cohort. **E–H** Representative images of RGMA protein expression examined by immunohistochemistry (IHC) staining in nontumorous breast tissues (**E**), ductal carcinoma in situ tissues (**F**), invasive ductal carcinoma without LNM (**G**) and invasive ductal carcinoma with LNM (**H**). **I** Area under the receiver operator characteristic (ROC) curve for RGMA in differential diagnosis of breast cancer with and without lymph node metastasis (AUC = 0.6614, $P = 0.003$). **J** and **K** Kaplan–Meier curves showed that patients with higher RGMA expression have better overall survival (OS)(**J**) and disease-free survival (DFS)(**K**) in 116 BC cohort. **L** The publicly accessible Kaplan–Meier Plotter database showed patients with higher RGMA expression have better relapse-free survival than patients with lower RGMA expression.

Table 1. Correlation between RGMA expression and clinicopathological features of 116 BC cohort.

Variable	n	RGMA expression		p
		Low	High	
Ages (years)				
≤40	17	10	7	0.473
>40, ≤60	82	38	44	
>60	17	10	7	
Lymph node metastases				
Negative	50	19	31	**0.024**
Positive	66	39	27	
pTNM stage				
I	23	6	17	0.081
II	49	27	22	
III	38	22	16	
IV	6	3	3	
pT stage				
T1	39	13	26	**0.012**
T2	70	39	31	
T3	7	6	1	
pN				
N0	50	19	31	0.118
N1	28	17	11	
N2	23	12	11	
N3	15	10	5	
Distant metastases				
M0	109	54	55	0.364
M1	7	4	3	
ER status				
Negative	28	20	8	**0.009**
Positive	88	38	50	
PR status				
Negative	27	20	7	**0.004**
Positive	89	38	51	
HER2 status				
Negative	75	34	41	0.174
Positive	41	24	17	
Molecular classification				
Luminal A	32	14	18	0.110
Luminal B	60	27	33	
HER-2+	11	8	3	
Triple-negative	6	5	1	
Missing	7	4	3	

Bold values indicate statistical significance P < 0.05.

Validation of RGMA in TCGA breast invasive carcinoma (BRCA) cohort was then chosen for further analysis of the relationship between its expression and clinicopathological parameters in TCGA cohort. As shown in Supplementary Table S4, the RGMA expression level was attenuated in older patients, and high RGMA expression was significantly correlated with negative lymph node metastasis and earlier T stage.

To further examine the prognostic values for RGMA in patients with BC, we implemented survival analysis using the data from the 116 patients. Kaplan–Meier survival curves showed that patients with high RGMA expression displayed favorable overall survival (OS, Fig. 1J) and disease-free survival (DFS, Fig. 1K). Moreover, to determine whether low RGMA expression was an independent prognostic factor for BC, we performed a univariate analysis followed by a multivariate cox proportional hazards analysis. The univariate analysis suggested that RGMA expression, lymph node metastasis, and tumor stage were significantly correlated with OS of BC patients (Table 2, $P < 0.05$), and multivariate analysis showed that RGMA expression was not an independent prognostic predictor for OS or DFS (HR = 0.461, 0.210–1.012 [95% CI], $P = 0.054$; and HR = 0.507, 0.224–1.151 [95% CI], $P = 0.104$; respectively); however, these data still supported RGMA as a protective factor (HR < 1) for patient survival.

Consistent with these results, using the publicly accessible Kaplan–Meier plotter bioinformatics analysis platform, we further showed that BC patients with elevated expression of RGMA exhibited better relapse-free survival (Fig. 1L). These findings demonstrated that RGMA served as a prognostic marker in BC.

DNMT1- and DNMT3A-mediated RGMA promoter hypermethylation results in the downregulation of RGMA in BC cells

As described in the preceding text, RGMA was downregulated in BC, and recent studies reveal that DNA methylation is an early event in the process of carcinogenesis and that it gradually increases during tumor progression [14]. A previous study reported that RGMA was frequently silenced by promoter methylation in colon cancer [10], and we thus hypothesized that promoter hypermethylation of RGMA would result in decreased expression in BC. Furthermore, using the UALCAN web-tool, we demonstrated that the promoter methylation level of RGMA in BC tissues was markedly increased compared with normal mammalian tissues (Fig. 1C). These data suggested that hypermethylation of the RGMA promoter contributed to the downregulation of RGMA expression in BC.

Based on a previous study [10] and bioinformatic analysis, the CpG site and primers for our methylation study were presented in Supplementary Fig. S1A. To select appropriate BC cell lines to study the function of RGMA, we selected T47D, MCF-7, MCF-7/ADM, MDA-MB-231, and MDA-MB-468 cells to examine RGMA expression. Our results showed higher mRNA and protein expression levels for RGMA in MDA-MB-468 cells than in T47D, MCF-7, MCF-7/ADM, or MDA-MB-231 cells, while RGMA expression in T47D and MCF-7 cells was reduced (Supplementary Fig. S1B and C).

MSP assays confirmed that MDA-MB-231 and MDA-MB-468 possessed low promoter methylation levels, whereas MCF-7/ADM and T47D cells exhibited enhanced levels (Fig. 2A). The demethylating agent 5-Aza-CdR significantly reversed RGMA promoter hypermethylation (Fig. 2B), and RT-qPCR and western blotting analyses revealed significantly elevated RGMA mRNA and protein expression levels after treatment with 5-Aza-CdR (Fig. 2C and D). Thus, DNA methylation appears key to inhibiting RGMA expression.

Given that DNA methyltransferases (DNMTs) are critical to DNA methylation, we explored the function of DNMT1, DNMT3A, and DNMT3B in RGMA methylation. First, we treated the BC cells with the demethylating agent 5-Aza-CdR, and compared with the control treatment, 5-Aza-CdR treatment significantly decreased DNMTs protein levels (Supplementary Fig. S1D–F). When we then analyzed the correlation between DNMTs and RGMA expression using TCGA data, we found that RGMA was inversely correlated with DNMT1, DNMT3A, and DNMT3B (Fig. 2E). Subsequent RT-qPCR and western blot assays of DNMT1 and DNMT3A knockdown depicted a significant increase in the expression of RGMA in T47D and MCF-7/ADM cells. Moreover, silencing DNMT3B expression also upregulated RGMA expression, but this difference was not as

Y. Li et al.

Table 2. Univariate and multivariate Cox proportional hazards regression analysis of overall survival and disease-free survival after surgery.

Variable	Univariate analysis			Multivariate analysis		
	P value	HR	95% CI	*P* value	HR	95% CI
Overall survival						
Age (≤40 vså 40, ≤60 vså 60)	0.811	1.092	0.533—2.234	0.321	1.475	0.684—3.179
LNM (negative vs positive)	**0.010**	3.311	1.333—8.196	0.738	1.180	0.444—3.135
pTNM (I vs II vs III vs IV)	**<0.0001**	3.708	2.173—6.329	**<0.0001**	3.888	2.161—6.994
RGMA expression (low vs high)	**0.046**	0.449	0.204—0.987	0.076	0.475	0.209—1.081
Disease-free survival						
Age (≤40vså 40, ≤60vså 60)	0.824	1.085	0.529—2.224	0.355	1.439	0.666—3.112
LNM (negative vs positive)	**0.010**	3.289	1.326—8.197	0.766	1.160	0.436—3.096
pTNM (I vs II vs III vs IV)	**<0.0001**	3.656	2.149—6.220	**<0.0001**	3.753	2.104—6.693
RGMA expression (low vs high)	0.054	0.461	0.210—1.012	0.104	0.507	0.224—1.151

Bold values indicate statistical significance P < 0.05.

notable (Fig. 2F and G). The interference efficiencies of si-DNMTs were controlled in RT-qPCR and western blot analysis (Supplementary Fig. S1G–O). Thus, we investigated the effects of DNMT1 and DNMT3A on RGMA methylation levels, and demonstrated that knockdown of DNMT1 and DNMT3A could reverse RGMA promoter methylation (Fig. 2H). ChIP assay further disclosed that DNMT1 and DNMT3A bound to the promoter region of RGMA (Fig. 2I–K). These results thus revealed that DNMT1- and DNMT3A-mediated RGMA promoter hypermethylation led to downregulation of RGMA expression in BC cells.

RGMA overexpression inhibits BC cell proliferation and colony formation and increases cellular apoptosis

To verify the functional significance of RGMA expression, we initially established overexpression of RGMA by cellular transfection with a pcDNA3.1-RGMA vector, using empty-vector transfection as a control, and verified transfection efficiency by western blot analysis (Fig. 3A). In our previous study, we demonstrated that RGMA inhibited cellular migration and invasion in BC [13], and in the present study, EdU assay indicated that RGMA overexpression notably inhibited DNA synthetic activities. Furthermore, CCK8 assay and colon formation assay revealed suppressed proliferation and colony formation by RGMA-overexpressing cells (Fig. 3B–F). Flow-cytometric assay also showed that RGMA overexpression resulted in enhanced apoptosis in BC cells (Fig. 3G and H). Overall, our findings supported the view that RGMA overexpression suppressed malignant proliferation and promoted apoptosis in BC cells.

RGMA knockdown promotes BC cell proliferation and colony formation and inhibits cell apoptosis

Lentivirus-mediated RGMA interference (LV-sh-RGMA) and short interference siRNAs directed against human RGMA (si-RGMA) were applied to knockdown the expression of RGMA, and knockdown efficiency was confirmed by western blotting (Fig. 4A). As shown in Fig. 4B, RGMA knockdown markedly increased DNA synthetic activities (Fig. 4B), and CCK8 assay demonstrated that RGMA knockdown promoted BC cell proliferation (Fig. 4C and D). Interestingly, RGMA knockdown effectively accelerated colony-formation abilities (Fig. 4E and F), and flow-cytometric assay revealed that RGMA knockdown reduced apoptotic rate in BC cells (Fig. 4G and H). Overall, our findings indicated that RGMA knockdown promoted malignant proliferation and colony formation and inhibited apoptosis of BC cells.

RGMA knockdown accelerates BC growth in vivo

In order to scrutinize the roles of RGMA in vivo, MDA-MB-231 cells transfected with LV-shRGMA/LV-shNC (and expressing GFP) were injected subcutaneously into the axillary fossa of mice, and we then examined the effects of 5-Aza-CdR on BC growth. Forty-five days later, when the xenograft tumors were harvested, we showed that xenograft tumor growth, tumor volume, and tumor weight were significantly augmented in the LV-shRGMA group compared to the LV-shNC group and that 5-Aza-CdR treatment suppressed tumor growth (Fig. 5A–D). In addition, tumor nodules in the LV-shRGMA group displayed more invasion of the margin and into the surrounding stroma or muscle tissues than LV-shNC group, while the tumors in the 5-Aza-CdR group were noninvasive and well-encapsulated (Fig. 5E). These results suggested that RGMA knockdown increased malignant growth and invasion by BC, while 5-Aza-CdR could reverse this phenomenon.

RGMA may function as a tumor suppressor by inhibiting the FAK/Src/PI3K/AKT/Bcl-2 signaling pathway

Since previous investigators reported that RGMA stimulation promoted focal adhesion kinase (FAK) dephosphorylation [15], we measured the effect of RGMA on the expression of total FAK protein and the phosphorylation levels of FAK. Our results demonstrated that phosphorylated FAK (p-FAK) was dramatically increased in BC cells showing RGMA knockdown, and while the total FAK protein level showed no change. We obtained opposing results in RGMA-overexpressing cells (Fig. 6A). We then extracted the protein from the xenograft tumors after LV-sh-RGMA and LV-sh-NC transfection and demonstrated that compared with the control group, the LV-sh-RGMA group displayed markedly higher p-FAK expression, with no major change in total FAK expression (Fig. 6B).

Several studies suggested that the FAK/Src protein-protein complex can activate the PI3K/AKT-signaling pathway and then promote cellular proliferation [16, 17]. Thus, we conjectured that RGMA inhibited tumor growth by modulating the FAK/Src/PI3K/AKT-signaling pathway, and explored key related molecules (Src, p-Src, PI3K, p-PI3K, AKT, and p-AKT) following RGMA knockdown or overexpression. Compared with negative controls (NC), cells manifesting RGMA-knockdown showed significantly elevated p-Src, p-PI3K, and p-AKT levels (Fig. 6A). In addition, when we further evaluated the relative expression of downstream effector proteins in the mouse xenograft tumors, we noted dramatically elevated p-FAK, p-Src, p-PI3K, and p-AKT expression in the LV-sh-RGMA group compared to the negative control group (Fig. 6B). In contradistinction, Src, PI3K, and AKT phosphorylation levels declined in BC cells upon RGMA overexpression, indicating that RGMA knockdown could effectively promote FAK phosphorylation and subsequently activate the FAK/Src/PI3K/AKT-signaling pathway.

Bcl-2 is a downstream effector of the AKT-signaling pathway and regulates cellular proliferation and apoptosis [18–20]. As we
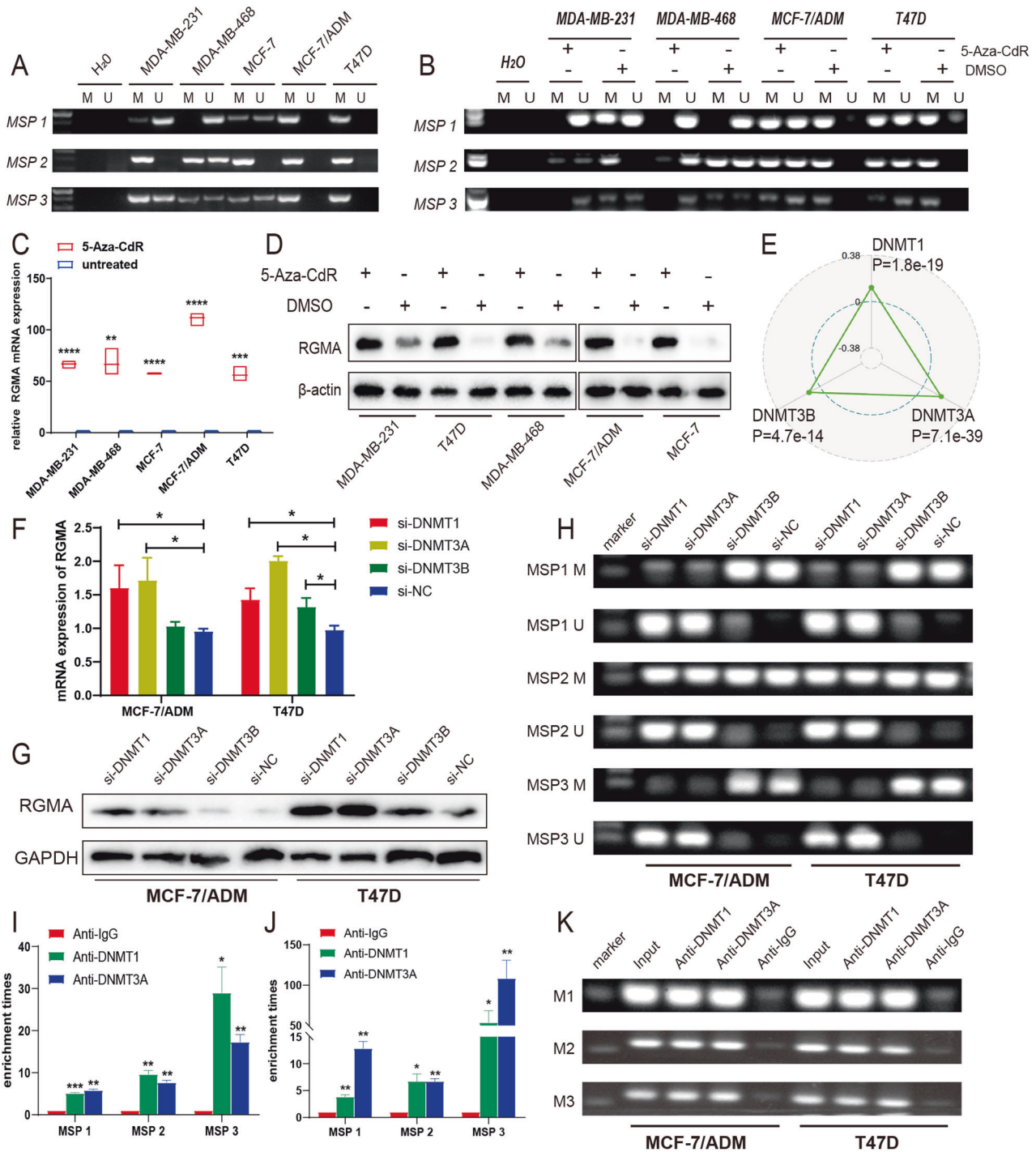
Fig. 2 **DNMT1 and DNMT3A-mediated RGMA promoter hypermethylation led to the RGMA downregulation in BC. A** Methylation specific PCR (MSP) analysis showed very frequent and variable extent of methylation of the RGMA gene promoters in five breast cancer cell lines. MDA-MB-231 and MDA-MB-468 possessed low promoter methylation levels, whereas MCF-7/ADM and T47D cells exhibited elevated levels. (M, methylation-specific PCR product; U, unmethylation-specific PCR). **B** After exposed to DNA methylation inhibitor, 5-Aza-CdR, the promoter methylation level of RGMA in BC cells was significantly decreased verified by MSP assay. **C**, **D** Treatment of 5-Aza-CdR significantly increased the RGMA mRNA (**C**) and protein (**D**) expression levels in BC cells. **E** The bioinformatics analysis showed that the expression of RGMA was inversely correlated with DNA methyltransferase (DNMT) family members (DNMT1, DNMT3A and DNMT3B) expression levels based on the TCGA database. **F** and **G** RGMA mRNA and protein expression was measured after BC cells treated with DNMT1 or DNMT3A or DNMT3B siRNA. DNMT1 and DNMT3A knockdown could significantly increase RGMA expression in T47D and MCF-7/ADM cells. Moreover, silencing DNMT3B expression also upregulated RGMA expression, but this difference was not as notable. **H** RGMA promoter methylation status was measured by MSP assay after BC cells transfected with DNMT siRNA. DNMT1 and DNMT3A knockdown could significantly reverse RGMA promoter methylation. In addition, DNMT3B knockdown also reversed RGMA promoter methylation, but this difference was not as notable. **I–K** ChIP assay demonstrated that DNMT1 and DNMT3A could bind to the promoter area of RGMA in MCF-7/ADM and T47D cells.
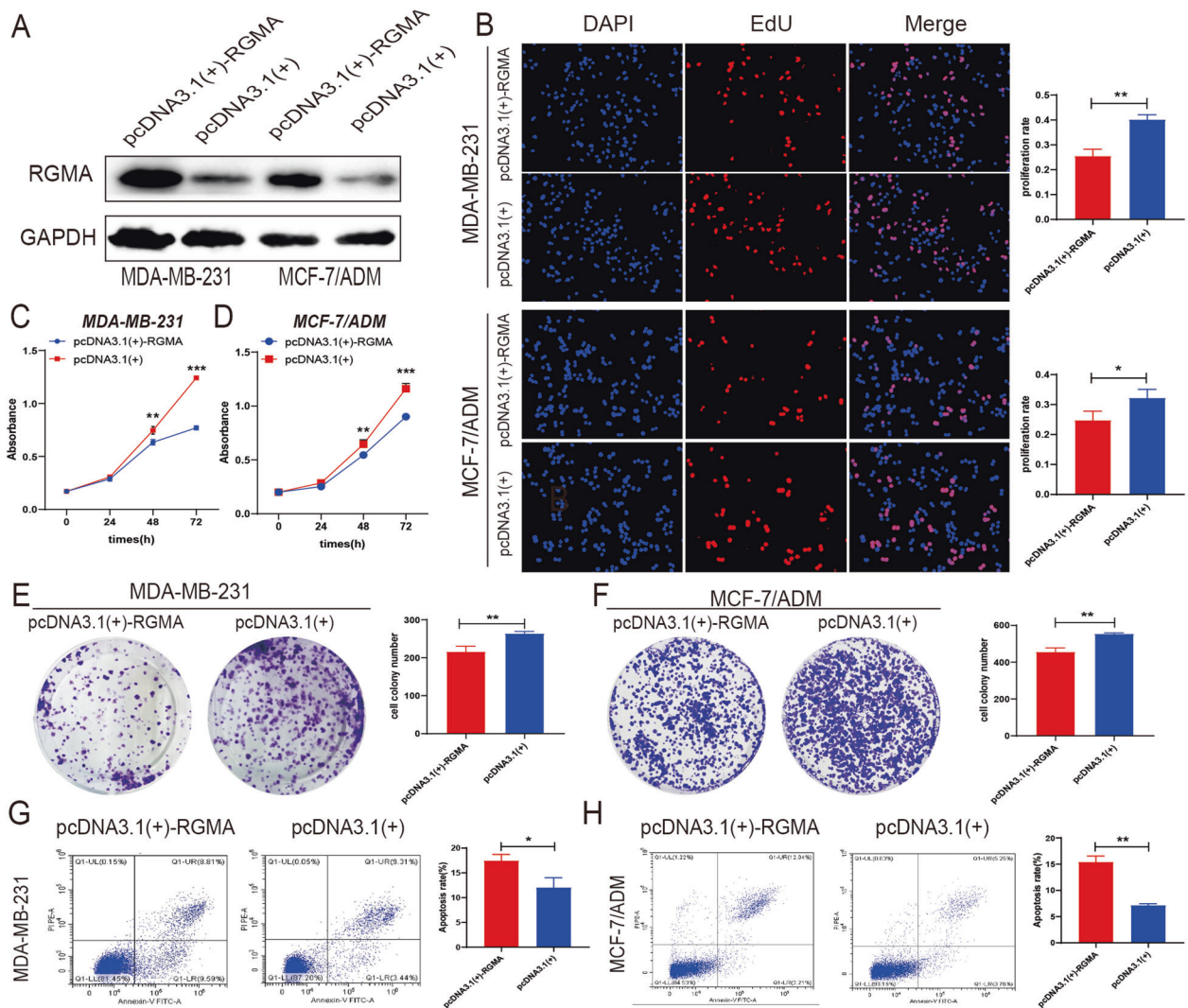
Fig. 3 RGMA overexpression inhibited BC cells proliferation and induced cell apoptosis. A Western blot analysis demonstrated the overexpression efficiency for the transfection of RGMA overexpression vector pcDNA3.1(+)-RGMA or pcDNA3.1-control. **B** EdU assays showed that RGMA overexpression inhibited DNA synthetic ability in BC cells. **C** and **D** CCK8 assays showed that RGMA overexpression inhibited cell proliferation in MDA-MB-231 and MCF-7/ADM cells. **E** and **F** Colony-formation assays showed that RGMA overexpression inhibited clone formation capability of BC cells. **G** and **H** Flow cytometry analysis indicated that RGMA overexpression induced cell apoptosis.

observed that RGMA was involved in BC cell proliferation and apoptosis, we further investigated the effects of RGMA on Bcl-2 expression. Accordingly, knockdown of RGMA upregulated Bcl-2 expression in BC cells, while Bcl-2 was downregulated in the RGMA-overexpressing cell lines (Fig. 6A and B). Collectively, these data indicated that knockdown of RGMA enhanced cancer cell proliferation and apoptotic resistance, which may have been in part due to activated FAK/Src/PI3K/AKT signaling and the subsequent upregulation of Bcl-2 expression.

As previously described, 5-Aza-CdR treatment inhibited BC cell growth via RGMA promoter hypermethylation, and we therefore further probed the effects of 5-Aza-CdR treatment on the RGMA/ FAK/Src/PI3K/AKT-signaling pathway in mouse xenograft tumors. Compared with NC, the 5-Aza-CdR group displayed markedly higher RGMA protein levels but dramatically lower levels of p-FAK, p-Src, p-PI3K, and p-AKT (Fig. 6B).

5′-Aza-CdR induces hypomethylation due to its ability to inhibit DNA methyltransferase activity and expression, and we herein demonstrated that DNMT1- and DNMT3A-mediated RGMA promoter hypermethylation led to downregulation of RGMA expression in BC cells. Thus, to further confirm that 5′-Aza-CdR

treatment-induced inactivation of the FAK/Src/PI3K/AKT-signaling pathway was dependent upon RGMA hypomethylation, we used si-DNMT1, si-DNMT3A, or 5′-Aza-CdR to inhibit DNMT1 and DNMT3A expression in LV-shRGMA cells or control LV-NC cells. Our results showed that RGMA hypermethylation and inhibition of RGMA expression could be reversed by DNMT siRNA or its specific inhibitor (5′-Aza-CdR), as these treatments partially reversed RGMA knockdown-induced activation of the FAK/Src/PI3K/AKT pathway in LV-shRGMA cells compared to control cells. (Fig. 2 and Fig. 6C). Given these findings, 5-Aza-CdR treatment restored RGMA expression by inhibiting DNMT1 and DNMT3A expression and inducing demethylation, which in turn further obstructed the FAK/ Src/PI3K/AKT-signaling pathway and contributed to the suppression of BC growth.

DISCUSSION

BC is a heterogeneous disease that exhibits diverse genetic alterations, and the identification of genes associated with malignant tumors might therefore be of great importance in cancer diagnosis and treatment [21]. In the present study, we
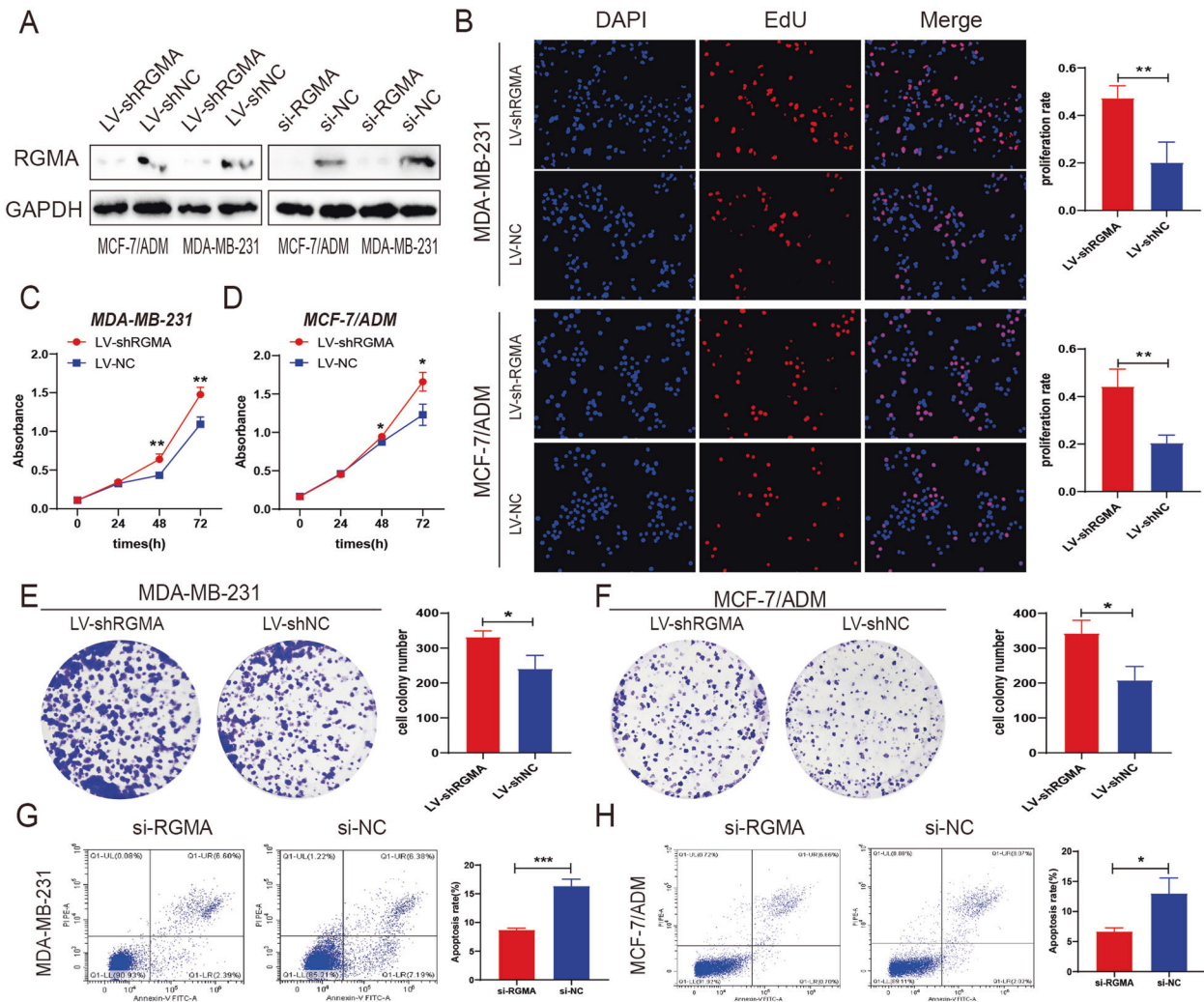
Fig. 4 RGMA knockdown promoted BC cells proliferation and suppressed cell apoptosis. A Western blot analysis demonstrated the knockdown efficiency for the transfection of RGMA lentivirus (LV-shRGMA), small interfering RNA (si-RGMA) or corresponding negative control (LV-shNC or si-NC). **B** EdU assays showed that RGMA knockdown promoted DNA synthetic ability in BC cells. **C** and **D** CCK8 assays showed that RGMA knockdown enhanced BC cells proliferation. **E** and **F** Colony-formation assays showed that RGMA knockdown enhanced clone formation capability of BC cells. **G** and **H** Flow cytometry analysis indicated that RGMA knockdown decreased BC cell apoptotic rate.

reported that DNMT1 and DNMT3A contributed to RGMA hypermethylation that led to the downregulation of RGMA in BC and that RGMA downregulation accelerated BC growth and apoptotic resistance through activation of the FAK/Src/PI3K/AKT-signaling pathway.

We posit that RGMA might be clinically recognized as a prognostic biomarker in BC, as its lowered expression indicated poorer prognosis for BC patients. Clinicopathologic parameter analysis revealed that a higher RGMA level was correlated with earlier T stage, negative lymph-node involvement, and positive ER and PR status. Even though the difference in RGMA expression between LNM and non-LNM groups was statistically significant, the small effect size (AUC = 0.66) signified that the model did not possess a robust capability to distinguish between the groups. These findings therefore need to be further examined in the future.

In the current study we also explored the effects of RGMA on BC, as our previous study showed that RGMA knockdown significantly promoted BC cell proliferation and migration [13]. We herein thus verified these phenomena, as EdU, colony-formation, and CCK8 assays suggested that RGMA knockdown significantly accelerated cancer cell proliferation. Xenograft animal experiments further confirmed that RGMA knockdown

contributed to subcutaneous tumor growth and that restoring RGMA expression by demethylation agents, 5-Aza-CdR, effectively suppressed tumor growth. Although these results implied that RGMA acts as a tumor suppressor in BC, little is known regarding the mechanisms underlying RGMA gene inactivation in BC.

The downregulation of RGMA expression in cancer cells is caused by various mechanisms, including loss of heterozygosity, promoter hypermethylation, and miRNA inhibition. Our previous study established that RGMA was a direct target of miR-4472 in BC [13], and RGMA was also shown to be regulated by miR-210-3p in oral squamous cell carcinoma [7]. Moreover, abnormal DNA methylation is common in epigenetic regulation as observed in tumorigenesis [14]. DNA methylation is mediated by DNMTs, including DNMT1, DNMT3A, and DNMT3B [22], and silencing of DNMT expression and inhibition of DNMT activity by DNA demethylating agents (5-Aza-CdR) prevents tumorigenesis [23, 24]. The present study suggests that the RGMA promoter is hypermethylated in BC, as knockdown of DNMT1 and DNMT3A resulted in the restoration of RGMA expression. Moreover, DNMT1 and DNMT3A can be recruited to the RGMA promoter in BC cells and then induce RGMA promoter-region hypermethylation. The DNA methyltransferase inhibitor 5-Aza-CdR has been shown to be
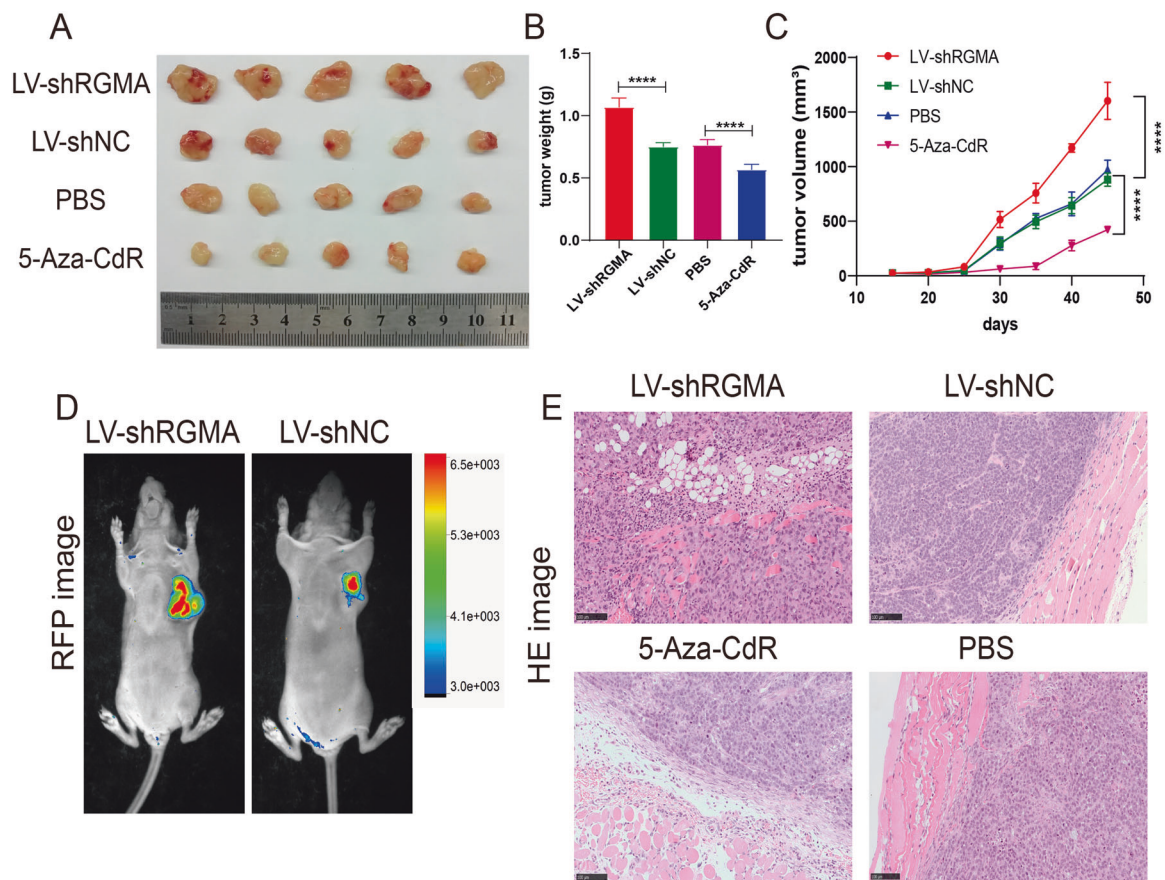
Fig. 5 Low expression of RGMA could accelerate tumor growth, while 5-Aza-CdR treatment could effectively inhibit tumor growth. A Photographs of dissected tumors from nude mice implanted with MDA-MB-231 cells pretreated with LV-shRGMA, LV-shNC, 5-Aza-CdR treatment and PBS treatment, respectively. **B** Average tumor weight of each group. RGMA knockdown could significantly promoted tumor growth in vivo, while 5-Aza-CdR treatment suppressed tumor tumorigenicity ability. **C** Tumor growth curves showed that RGMA knockdown accelerated tumor malignant growth, while treatment with 5-Aza-CdR could slow the rate of tumor growth in vivo. **D** The tumors were imaged by in vivo imaging system. **E** Tumor xenografts from nude mice were used for hematoxylin-eosin (HE) staining. The xenograft tumors of LV-shRGMA group displayed more local invasion, whereas the tumors of LV-shNC group were non-invasive and the 5-Aza-CdR group showed more well-encapsulated. Scale bars, 100 μm.

efficient in promoting the chemotherapeutic efficacy of BC [25], and 5-Aza-CdR improves the chemosensitivity of anticancer drugs and serves as a potential therapeutic target for BC management [25]. 5-Aza-CdR treatment also restores PKD1 expression via reversal of PRKD1 promoter methylation and blocks breast tumor spread and metastasis to the lung in a PKD1-dependent fashion [26]. Consistent with previous studies, our investigation revealed that 5-Aza-CdR treatment effectively suppressed DNMT1 and DNMT3A expression, which further restored RGMA expression and inhibited breast tumor growth. Collectively, these findings suggest that 5-Aza-CdR treatment constitutes a promising clinical therapeutic target in BC by reactivating the expression of silenced tumor-suppressor genes.

Investigators previously demonstrated that RGMA stimulation promoted FAK dephosphorylation [15]. FAK is a cytoplasmic tyrosine kinase that is important in cellular proliferation and migration [27], and Src interacts with FAK to form a FAK/Src complex. Moreover, the FAK/Src complex initiates recruitment of phosphoinositide 3-kinase (PI3K), which further activates AKT signaling and stimulates malignant progression of cancer [28]. In this study, low RGMA expression promoted the activation of the FAK/Src/PI3K/AKT-signaling pathway and contributed to malignant growth and apoptotic resistance of BC. Furthermore, rescue experiments revealed that 5-Aza-CdR treatment or si-DNMT transfection increased RGMA expression levels and partially abrogated RGMA knockdown-induced activation of the FAK/Src/

PI3K/AKT pathway in LV-shRGMA cells compared to control cells. Therefore, 5-Aza-CdR can restore RGMA expression by reversing the highly methylated state of the RGMA gene promoter by inhibiting DNMT1 and DNMT3A expression and reversing the mobilization of the FAK/Src/PI3K/AKT pathway.

In summary, we herein demonstrated for the first time that DNMT1- and DNMT3A-mediated RGMA promoter hypermethylation leads to downregulation of RGMA expression in BC and that low RGMA expression contributes to malignant progression via activation of the FAK/Src/PI3K/AKT-signaling pathway. 5-Aza-CdR treatment inhibited DNMT1 and DNMT3A expression and reversed RGMA promoter methylation, which further reactivated the expression of the tumor suppressor RGMA, thereby blocking tumor growth. Collectively, our data showed that RGMA might serve as a promising therapeutic target in the treatment of BC.

METHODS
Human BC samples
A total of 116 patient tumor samples that were pathologically diagnosed as BC were collected from Qilu Hospital of Shandong University, China, from June 2004 to December 2011. None of the patients had received any form of neo-adjuvant therapy prior to surgery. This study was approved by the Ethical Committee on Scientific Research of Shandong University Qilu Hospital, and informed consent was obtained from all recruited patients. We obtained expression information from The Cancer Genome Atlas
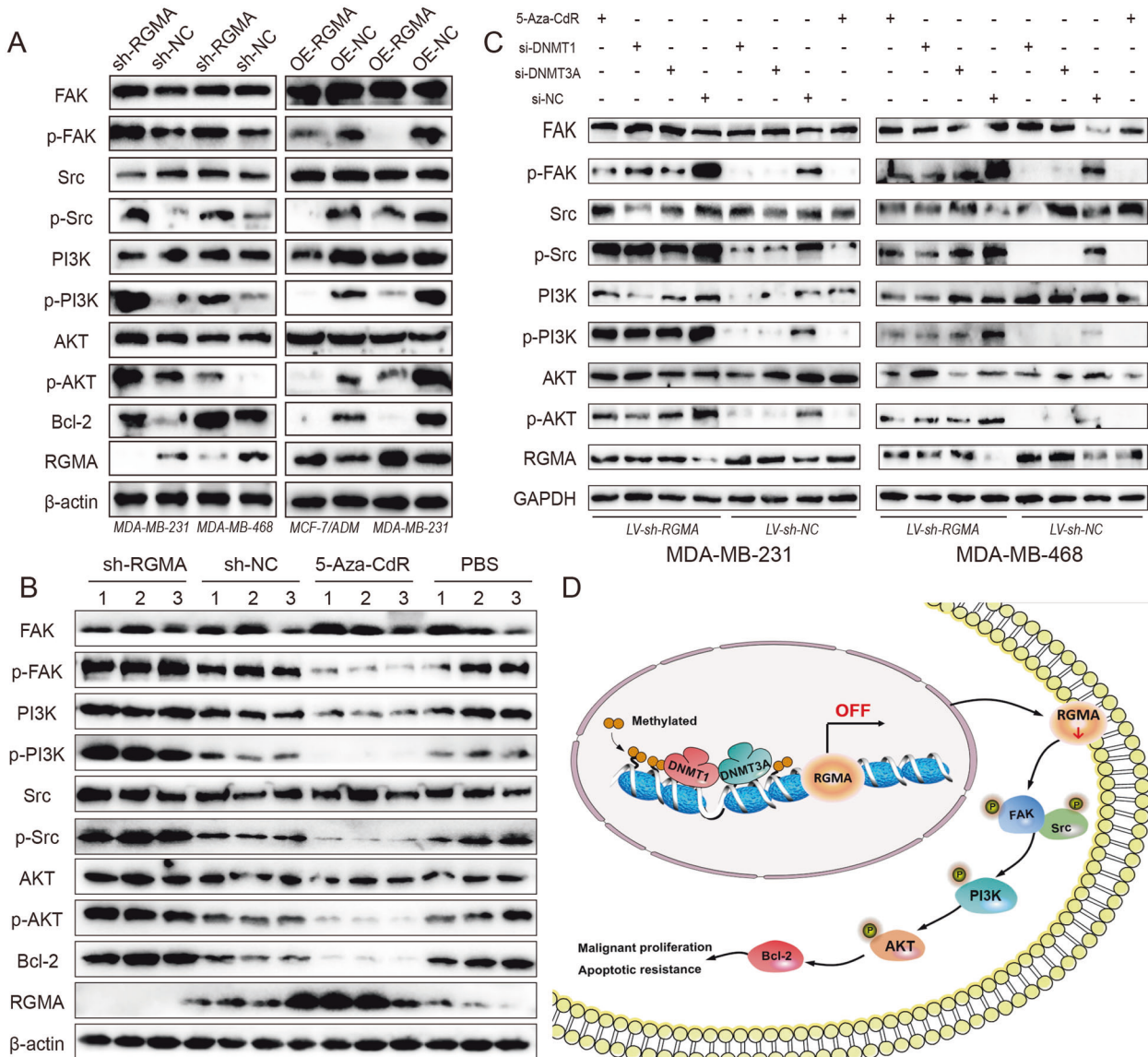
Fig. 6 RGMA exerted function in BC cells via FAK/Src/PI3K/AKT signaling pathway. A The protein level of the FAK/Src/PI3K/AKT signaling pathway related markers in BC cells after treated with RGMA overexpression vector or LV-sh-RGMA. The FAK/Src/PI3K/AKT signaling pathway was activated in sh-RGMA cells, while the opposing results were shown in RGMA-overexpressing cells. **B** Western blot analyses of the xenograft tumors protein showed that RGMA knockdown activated FAK/Src/PI3K/AKT signaling pathway, while 5-Aza-CdR treatment suppressed the activation via restoring RGMA expression. **C** Western blot assay demonstrated that siDNMT1 or si-DNMT3A or 5′-Aza-CdR could inhibit DNMT1 and DNMT3A expression in LV-shRGMA cells or control LV-shNC cells, which restored RGMA expression and further suppressed FAK/Src/PI3K/AKT signaling pathway activation. **D** Schematic illustration of the molecular mechanism of RGMA in BC. DNMT1 and DNMT3A-mediated RGMA promoter hypermethylation leads to downregulation of RGMA expression in BC, and low RGMA expression contributes to malignant progression via activation of FAK/Src/PI3K/AKT signaling pathway.

(TCGA) for RGMA using UALCAN (http://ualcan.path.uab.edu/index.html) [29], and the Kaplan–Meier plotter database (www.kmplot.com) [30] was used to verify the association between RGMA expression and prognosis in BC patients.

Immunohistochemistry (IHC)

Paraffin-embedded tissues were sectioned, dewaxed, and subjected to high temperature-antigen retrieval in EDTA antigenic-retrieval buffer for 10 min. Following incubation with 3% H_2O_2, the tissues were blocked with normal goat serum for 30 min and then incubated with primary antibody for RGMA (1:100 dilution; Abcam, Danvers, MA, USA) overnight at 4 °C. Afterward, the sections were incubated with biotin-labeled secondary antibody for 30 min, followed by horseradish peroxidase-labeled streptavidin solution at room temperature for 20 min. Finally, the tissues were stained with DAB, rinsed with distilled water, and

counterstained with hematoxylin. RGMA expression was semi-quantitatively evaluated as previously reported [31]. The staining intensities and the corresponding percentages were independently evaluated by two professional pathologists. RGMA staining intensity was classified as follows: weak (1 point), moderate (2 points), or strong (3 points). Staining scores were then calculated as follows: score (maximum of 300) = (1 × percentage of weakly staining cells) + (2 × percentage of moderately staining cells) + (3 × percentage of strongly staining cells). Median scores were selected as thresholds to separate low- and high-expression groups.

Cell lines and cell culture

Human MDA-MB-231, MDA-MB-468, T47D, MCF-7 and MCF-7/ADM (resistant to Adriamycin) cell lines were used. The detailed culture condition was described in Supplementary Methods.

Cell transfection

The RGMA small interfering RNA (siRNA), DNMT1 siRNA, DNMT3A siRNA, DNMT3B siRNA or respective NC were purchased from GenePharma (Shanghai, China). The sequence was listed in Supplementary Table S1 [32]. These were transfected into cells using X-tremeGENE transfection reagents (Roche, IN, U.S.), according to the manufacturer's instructions. The full-length cDNA sequence of RGMA was cloned into the expression plasmid pcDNA3.1 (+) (pcDNA3.1 (+) -RGMA) and the empty plasmid pcDNA3.1 (+) was used as a control [13]. Plasmids were transfected with TurboFect™ Transfection Reagent (Invitrogen, USA).

Lentivirus infection

The RGMA-silencing lentivirus (LV-shRGMA) and negative control lentivirus (LV-shNC) were constructed by GenePharma (Shanghai, China). The sequence was listed in Supplementary Table S1. BC cells were seeded in six-well plates, grown overnight, and then infected with lentivirus. The infection rate of lentivirus was determined by fluorescence microscopy 72 h after infection. Puromycin (2 ug/mL) was added to the medium to kill the uninfected cells.

RNA isolation and RT-qPCR assays

Total RNA was extracted with Trizol reagents (Invitrogen, Carlsbad, CA) and the mRNA expression levels were evaluated by real-time quantitative PCR (RT-qPCR). Total RNA was reverse-transcribed to cDNA using a Reverse Transcription Kit (Toyobo Co., Ltd. Japan) and RT-qPCR was performed using a SYBR Green PCR Kit (Takara, Japan). The sequences of the primers were described in Supplementary Table S2.

Cell proliferation and colony formation assays

Cell proliferation was performed using CCK8, EdU and colony formation assay as previously described [13, 16]. The details were given in Supplementary Methods.

Cell apoptosis assay

Cell apoptosis assay was assessed using an Annexin V-FITC/PI Apoptosis Detection Kit (BestBio, Shanghai, China) as described in a previous study [13].

Western blot analysis

Cells were collected and lysed in RIPA buffer. Then the lysates were separated by 10% SDS-polyacrylamide gel electrophoresis, transferred to polyvinylidene difluoride membranes and blotted with primary antibodies against RGMA (1:1000, Abcam, Cambridge, UK), FAK (1:1000, Abcam), p-FAK (1:1000, Abcam), Src (1:1000, Abcam), p-Src (1:1000, Abcam), PI3K (1:1000, Abcam), p-PI3K (1:1000, Abcam), AKT (1:1000, Abcam), p-AKT (1:1000, Abcam), Bcl-2 (1:1000, Abcam), β-actin (1:5000, Abcam) and GAPDH (1:5000, Abcam). The bands detected by an ECL Western Blotting Detection Reagent (Merck Millipore, Darmstadt, Germany).

Methylation-specific PCR (MSP)

To perform the MSP assay, DNA was purified and underwent modification using sodium bisulfite, which converts all unmethylated cytosine to uracil, leaving methylated cytosine unchanged. The MSP experiment required two pairs of primers: One pair was specific for methylated DNA (M) and the other for unmethylated DNA (U). Successful amplification from the M primer pair was indicative of methylated DNA, and a PCR product of a U primer pair was representative of unmethylated DNA [33]. Genomic DNA was extracted from five BC cell lines using a TIANamp genomic DNA kit (Tiangen, Beijing, China). Approximately 1 μg of extracted DNA was subjected to bisulfite conversion using a CpGenome DNA modification kit (Intergen Co., Purchase, NY) according to the manufacturer's instructions. Bisulfite-converted DNA was then used as template for PCR using a Taq hot-start polymerase (TaKaRa, Japan). The three MSP pairs of primers spanning different regions of the RGMA promoter are listed in Supplementary Table S3. The resulting PCR products were separated on 1% agarose gels.

5-aza-2-deoxycytidine (5-Aza-CdR) treatment

BC cells were seeded into 12-well plates 16 h before treatment with 5 μmol/L 5-Aza-CdR (Sigma, St. Louis, MO) for 3 days. After treatment, the culture medium was removed, and RNA and DNA were extracted as previously described.

Chromatin immunoprecipitation (ChIP) assay

ChIP assay was performed with the SimpleChIP® Plus Enzymatic Chromatin IP Kit (Cell Signaling Technology, USA) according to the manufacturer's instructions. Briefly, BC cells were cross-linked in PBS containing 1% formaldehyde at room temperature for 10 min. Then the cross-linked chromatin DNA was destroyed by sonication. The chromatin was then immunoprecipitated using an anti-DNMT1 and anti-DNMT3A antibody. Normal mouse IgG was used as the negative control. The ChIP-enriched DNA was analyzed by PCR.

Tumor xenograft model

To evaluate in vivo tumorigenicity, we established subcutaneous BC animal xenograft models. MDA-MB-231 cells (1×10^7) stably transfected with LV-shRGMA or LV-shNC were subcutaneously injected into the right flanks of 4-week-old BALB/c nude mice ($n = 5$ per group, allocated randomly). For treatments with 5-Aza-CdR, MDA-MB-231 cells were exposed to 500 nM 5-Aza-CdR (Selleck, Texas, American) for 4 days, and then the 5-Aza-CdR- or PBS-treated cells were subcutaneously injected into the right flanks of 4-week-old BALB/c nude mice ($n = 5$ per group, allocated randomly). They were treated with 5-Aza-CdR (2.5 mg/kg) or PBS by intraperitoneal injection once every 3 days, and their tumor volumes were monitored every 5 days. The tumor volume was calculated as volume = (width^2 × length) ÷ 2. After 7 weeks, the mice were sacrificed, and xenografts were removed. The animal experiments were approved by the Shandong University Animal Care and Use Committee, and conducted in a blinded manner.

Statistical analysis

GraphPad Prism 8.0 (GraphPad Software, San Diego, CA) was used for statistical analysis. A student's t test and one-way ANOVA were used to determine the significance of two groups and multiple groups, respectively. A chi-square test and a Fisher's exact test were used to determine the relationship between RGMA and clinicopathological variables. Spearman correlation was used to determine the correlation between tumor size and RGMA expression ($p < 0.05$ were considered statistically significant).

DATA AVAILABILITY

All data generated or analyzed during this study are included in this published article and its supplementary information files.

REFERENCES

1. Bray F, Ferlay J, Soerjomataram I, Siegel RL, Torre LA, Jemal A. Global cancer statistics 2018: GLOBOCAN estimates of incidence and mortality worldwide for 36 cancers in 185 countries. CA Cancer J Clin. 2018;68:394–424.
2. Schoeps A, Rudolph A, Seibold P, Dunning AM, Milne RL, Bojesen SE, et al. Identification of New Genetic Susceptibility Loci for Breast Cancer Through Consideration of Gene-Environment Interactions. Genet Epidemiol. 2014;38:84–93.
3. Abdel-Hafiz HA, Horwitz KB. Role of epigenetic modifications in luminal breast cancer. Epigenomics. 2015;7:847–62.
4. Siebold C, Yamashita T, Monnier PP, Mueller BK, Pasterkamp RJ. RGMs: Structural Insights, Molecular Regulation, and Downstream Signaling. Trends Cell Biol. 2017;27:365–78.
5. O'Leary C, Cole SJ, Langford M, Hewage J, White A, Cooper HM. RGMa regulates cortical interneuron migration and differentiation. PLoS ONE. 2013;8:e81711.
6. Korecka JA, Moloney EB, Eggers R, Hobo B, Scheffer S, Ras-Verloop N, et al. Repulsive Guidance Molecule a (RGMa) Induces Neuropathological and Behavioral Changes That Closely Resemble Parkinson's Disease. J Neurosci. 2017;37:9361–79.
7. Lu Y, Li Y, Wang Z, Xie S, Wang Q, Lei X, et al. Downregulation of RGMA by HIF-1A/miR-210-3p axis promotes cell proliferation in oral squamous cell carcinoma. Biomed Pharmacother. 2019;112:108608.
8. Zhao ZW, Lian WJ, Chen GQ, Zhou HY, Wang GM, Cao X, et al. Decreased expression of repulsive guidance molecule member A by DNA methylation in colorectal cancer is related to tumor progression. Oncol Rep. 2012;27:1653–9.
9. Li J, Ye L, Kynaston HG, Jiang WG. Repulsive guidance molecules, novel bone morphogenetic protein co-receptors, are key regulators of the growth and aggressiveness of prostate cancer cells. Int J Oncol. 2012;40:544–50.
10. Li VSW, Yuen ST, Chan TL, Yan HHN, Law WL, Yeung BHY, et al. Frequent Inactivation of Axon Guidance Molecule RGMA in Human Colon Cancer Through Genetic and Epigenetic Mechanisms. Gastroenterology. 2009;137:176–87.
11. Zhang G, Wang R, Cheng K, Li Q, Wang Y, Zhang R, et al. Repulsive Guidance Molecule a Inhibits Angiogenesis by Downregulating VEGF and Phosphorylated Focal Adhesion Kinase In Vitro. Front Neurol. 2017;8:504.

12. Xiao B, Chen L, Ke Y, Hang J, Cao L, Zhang R, et al. Identification of methylation sites and signature genes with prognostic value for luminal breast cancer. BMC Cancer. 2018;18:405.

13. Li Y, Wang YW, Chen X, Ma RR, Guo XY, Liu HT, et al. MicroRNA-4472 Promotes Tumor Proliferation and Aggressiveness in Breast Cancer by Targeting RGMA and Inducing EMT. Clin Breast Cancer. 2020;20:e113–26.

14. Klutstein M, Nejman D, Greenfield R, Cedar H. DNA Methylation in Cancer and Aging. Cancer Res. 2016;76:3446–50.

15. Endo M, Yamashita T. Inactivation of Ras by p120GAP via focal adhesion kinase dephosphorylation mediates RGMa-induced growth cone collapse. J Neurosci. 2009;29:6649–62.

16. Li Y, Li X-Y, Li L-X, Zhou R-C, Sikong Y.GuX, et al. S100A10 Accelerates Aerobic Glycolysis and Malignant Growth by Activating mTOR-Signaling Pathway in Gastric Cancer. Front Cell Dev Biol. 2020;8:559486.

17. Niit M, Hoskin V, Carefoot E, Geletu M, Arulanandam R, Elliott B, et al. Cell-cell and cell-matrix adhesion in survival and metastasis: Stat3 versus Akt. Biomol Concepts. 2015;6:383–99.

18. Feng FB, Qiu HY. Effects of Artesunate on chondrocyte proliferation, apoptosis and autophagy through the PI3K/AKT/mTOR signaling pathway in rat models with rheumatoid arthritis. Biomed Pharmacother. 2018;102:1209–20.

19. Jia X, Wen Z, Sun Q, Zhao X, Yang H, Shi X, et al. Apatinib suppresses the Proliferation and Apoptosis of Gastric Cancer Cells via the PI3K/Akt Signaling Pathway. J BUON. 2019;24:1985–91.

20. Bao RK, Zheng SF, Wang XY. Selenium protects against cadmium-induced kidney apoptosis in chickens by activating the PI3K/AKT/Bcl-2 signaling pathway. Environ Sci Pollut Res Int. 2017;24:20342–53.

21. Zhang Y, He W, Zhang S. Seeking for Correlative Genes and Signaling Pathways With Bone Metastasis From Breast Cancer by Integrated Analysis. Front Oncol. 2019;9:138.

22. Subramaniam D, Thombre R, Dhar A, Anant S. DNA methyltransferases: a novel target for prevention and therapy. Front Oncol. 2014;4:80.

23. Pathania R, Ramachandran S, Mariappan G, Thakur P, Shi H, Choi JH, et al. Combined Inhibition of DNMT and HDAC Blocks the Tumorigenicity of Cancer Stem-like Cells and Attenuates Mammary Tumor Growth. Cancer Res. 2016;76:3224–35.

24. Pathania R, Ramachandran S, Elangovan S, Padia R, Yang P, Cinghu S, et al. DNMT1 is essential for mammary and cancer stem cell maintenance and tumorigenesis. Nat Commun. 2015;6:6910.

25. Mirza S, Sharma G, Pandya P, Ralhan R. Demethylating agent 5-aza-2-deoxycytidine enhances susceptibility of breast cancer cells to anticancer agents. Mol Cell Biochem. 2010;342:101–9.

26. Borges S, Doppler H, Perez EA, Andorfer CA, Sun Z, Anastasiadis PZ, et al. Pharmacologic reversion of epigenetic silencing of the PRKD1 promoter blocks breast tumor cell invasion and metastasis. Breast Cancer Res. 2013;15:R66.

27. Schaller MD. Cellular functions of FAK kinases: insight into molecular mechanisms and novel functions. J Cell Sci. 2010;123:1007–13. Pt 7

28. Luo M, Guan JL. Focal adhesion kinase: a prominent determinant in breast cancer initiation, progression and metastasis. Cancer Lett. 2010;289:127–39.

29. Chandrashekar DS, Bashel B, Balasubramanya SAH, Creighton CJ, Ponce-Rodriguez I, Chakravarthi B, et al. UALCAN: a Portal for Facilitating Tumor Subgroup Gene Expression and Survival Analyses. Neoplasia. 2017;19:649–58.

30. Gyorffy B, Lanczky A, Eklund AC, Denkert C, Budczies J, Li Q, et al. An online survival analysis tool to rapidly assess the effect of 22,277 genes on breast cancer prognosis using microarray data of 1,809 patients. Breast Cancer Res Treat. 2010;123:725–31.

31. Specht E, Kaemmerer D, Sanger J, Wirtz RM, Schulz S, Lupp A. Comparison of immunoreactive score, HER2/neu score and H score for the immunohistochemical evaluation of somatostatin receptors in bronchopulmonary neuroendocrine neoplasms. Histopathology. 2015;67:368–77.

32. Liu H, Song Y, Qiu H, Liu Y, Luo K, Yi Y, et al. Downregulation of FOXO3a by DNMT1 promotes breast cancer stem cell properties and tumorigenesis. Cell Death Differ. 2020;27:966–83.

33. Ku JL, Jeon YK, Park JG. Methylation-specific PCR. Methods Mol Biol. 2011;791:23–32.

AUTHOR CONTRIBUTIONS
PG, YXZ and YL conceived the study; YL, HTL, XC, YWW, YRT, RRM and LS performed the experiments; YL analyzed the data and wrote the paper; YL, HTL and PG revised the paper. All authors have read and approved the final paper.

COMPETING INTERESTS
The authors declare no competing interests.

ETHICS APPROVAL AND CONSENT TO PARTICIPATE
This study was approved by the Ethical Committee on Scientific Research of Shandong University.

ADDITIONAL INFORMATION
Supplementary information The online version contains supplementary material available at https://doi.org/10.1038/s41388-021-02083-y.

Correspondence and requests for materials should be addressed to Yong-Xin Zou or Peng Gao.

Reprints and permission information is available at http://www.nature.com/reprints

Publisher's note Springer Nature remains neutral with regard to jurisdictional claims in published maps and institutional affiliations.